**This is an Accepted Manuscript of an article published by Taylor & Francis Group in Environmental Technology on 19 Sep 2018, available online: https://doi.org/10.1080/09593330.2018.1518994**

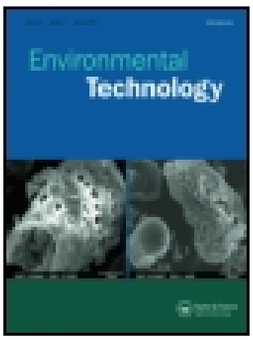

Environmental Technology

ISSN: 0959-3330 (Print) 1479-487X (Online) Journal homepage: http://www.tandfonline.com/loi/tent20

# Treatment of tequila vinasse and elimination of phenol by coagulation-flocculation process coupled with heterogeneous photocatalysis using titanium dioxide nanoparticles

Alicia Rodriguez Arreola, Marciano Sanchez Tizapa, Florentina Zurita, Juan Pablo Morán-Lázaro, Rocío Castañeda Valderrama, José Luis Rodríguez-López & Alejandra Carreon-Alvarez

**To cite this article:** Alicia Rodriguez Arreola, Marciano Sanchez Tizapa, Florentina Zurita, Juan Pablo Morán-Lázaro, Rocío Castañeda Valderrama, José Luis Rodríguez-López & Alejandra Carreon-Alvarez (2018): Treatment of tequila vinasse and elimination of phenol by coagulation-flocculation process coupled with heterogeneous photocatalysis using titanium dioxide nanoparticles, Environmental Technology, DOI: 10.1080/09593330.2018.1518994

**To link to this article:** https://doi.org/10.1080/09593330.2018.1518994

Accepted author version posted online: 01 Sep 2018.

**Publisher:** Taylor & Francis & Informa UK Limited, trading as Taylor & Francis Group
**Journal:** *Environmental Technology*
**DOI:** 10.1080/09593330.2018.1518994



# Treatment of tequila vinasse and elimination of phenol by coagulation-flocculation process coupled with heterogeneous photocatalysis using titanium dioxide nanoparticles

Alicia Rodriguez Arreola[1], Marciano Sanchez Tizapa[1], Florentina Zurita[2], Juan Pablo Morán-Lázaro[1], Rocío Castañeda Valderrama[1], José Luis Rodríguez-López[3], Alejandra Carreon-Alvarez[1,*]

[1]*Departamento de Ciencias Exactas y Naturales. Centro Universitario de los Valles. Universidad de Guadalajara. Carretera Guadalajara-Ameca Km. 45.5, C.P. 46600, Ameca, Jalisco, México.*

[2]*Departamento de Ciencias Tecnológicas. Centro Universitario de la Ciénega. Universidad de Guadalajara. Av. Universidad 1115. Col. Lindavista, Ocotlán, Jal.*

[3]*División de Materiales Avanzados. Instituto Potosino de Investigación Científica y Tecnológica A.C (IPICyT). Camino a la Presa de San José 2055, Lomas 4 Sección, C.P. 78216 San Luis, S. L. P.*

*ale_carreon_a@yahoo.com.mx

# Treatment of tequila vinasse and elimination of phenol by coagulation-flocculation process coupled with heterogeneous photocatalysis using titanium dioxide nanoparticles.

In this research we are reporting the treatment of tequila vinasse by a coagulation-flocculation process coupled with heterogeneous photocatalysis using two types of titanium dioxide nanoparticles, i.e., 1) commercial nanoparticles, and 2) nanoparticles synthesized by sol-gel. The efficiency in the elimination of phenol, which is one of the most harmful contaminants in tequila vinasse, was also included in the evaluation of the treatment process. The synthesized titanium dioxide nanoparticles were annealed in air at 400°C for 1 h and were characterized by X-ray diffraction, transmission electron microscopy, ultraviolet-visible and Raman spectroscopy. Anatase phase was observed in both samples, with a crystallite size of 22.5 and 9.8 nm for commercial and synthesized nanoparticles respectively. Tequila vinasse was characterized before and after the treatments by measuring physicochemical parameters such as pH, chemical oxygen demand (COD), color, total suspended solids (TSS), as well as using ultraviolet-visible spectroscopy and Raman spectroscopy to identify the presence of organic compounds, and gas chromatography for phenol quantification. Raw vinasse was treated initially by coagulation-flocculation producing clarified vinasse, which in turn was treated by photocatalysis for 3 h using hydrogen peroxide as oxidizing agent. The use of synthesized titanium dioxide nanoparticles allowed the highest efficiencies, reaching reductions of 99.4 %, 86.0 % and 70.0 % for TSS, color, and COD respectively. Gas chromatography results showed the reduction of phenol concentrations in 89.7 % with our synthesized nanoparticles in contrast to 82.7 % reduction, with commercial titanium dioxide nanoparticles.

Keywords: Heterogeneous photocatalysis, Phenol, Titania nanoparticles, Tequila vinasse, Sol-gel

## 1. Introduction

Tequila vinasse is a harmful residual waste of tequila industries [1] as 9-14 liters of vinasse are generated per one tequila liter [2]. In 2014 1,763 millions of liters of vinasse were produced in the State of Jalisco, México, representing 88,145.50 tons of organic matter, which is equivalent to the annual contamination produced by 4’829,880 residents [3]; the production of tequila vinasse is one hundred times more harmful than

domestic residues [4]. Physicochemical parameters of this type of vinasse are 50000-150000 mg.$L^{-1}$ of COD, 30-70 % of biological oxygen demand (BOD), temperatures of 80-90°C, pH of 3-5 and settleable solids concentrations of ~39910 mg.$L^{-1}$. Tequila vinasse also contains poorly biodegradable or toxic organic compounds such as phenolic compounds, brown polymers (melanoidin), as well as high concentrations of potassium, and a variety of heavy metals [2]. Tequila vinasse is usually discharged into rivers and soils, producing serious pollution problems such as soil salinization and impermeabilization [3,5,6].

Some vinasses similar to tequila vinasse have been treated using physicochemical treatments, such as coagulation-flocculation [3], biopolymers [7], aerobic and anaerobic treatments [8,9], etc. However the best results have been observed using combined treatments, e.g., electrochemical treatments [10] with advanced oxidation processes (AOPs) such as ultraviolet visible (UV) radiation, adding hydrogen peroxide ($H_2O_2$) or ozone, photocatalysis (using $TiO_2$ or other metal oxides), Fenton reactions and photo-Fenton [11,12].

On the other hand, in AOPs, hydroxyl free radicals with strong oxidative potential are produced by irradiation of some semiconductors such as titanium dioxide ($TiO_2$). $TiO_2$ catalyst is one of the most studied materials in photocatalysis due to its characteristics such as high photocatalytic activity, low cost, low toxicity, high stability [13], ability to degrade several organic pollutants [14], e.g., aromatic compounds [15]. $TiO_2$ presents three allotropic crystalline phases: brookite (orthorhombic), anatase (tetragonal) and rutile (tetragonal), among them all, anatase has shown the highest catalytic activity. It has been found that the photocatalytic activity of a material depends on the structural and surface properties of the catalyst such as the band gap, particle size, crystalline phase, morphology, etc. [4].

Padilla de Souza et. al. (2013) investigated the treatment of sugar cane vinasse by a coagulation-flocculation process coupled with heterogeneous photocatalysis using $TiO_2$-P25, finding that the COD was reduced up to 80 % [16]. In another report, the same authors investigated the treatment of sugar cane vinasse by the same methods but comparing the effectiveness of $TiO_2$-P25 with that of $TiO_2$-Kronos and concluded that both catalysts reduced the COD [15]. In another similar study, Vieneetha et al (2013) investigated the treatment of alcohol vinasse by heterogeneous photocatalysis using Aeroxide-P25 $TiO_2$ nanoparticles in combination with $H_2O_2$, obtaining reductions of 60 and 75 % for COD and color, respectively [17].

As it has been shown above, the reports presented so far, were carried out for effluents similar to tequila vinasse, therefore this is the first work that reports the use of photocatalysis for the treatment of tequila vinasse. The first objective of this research was to evaluate the tequila vinasse treatment by a process of coagulation-flocculation coupled with heterogeneous photocatalysis using titanium dioxide nanoparticles synthesized by sol-gel; while the second objective was to compare the performance of commercial $TiO_2$, versus $TiO_2$ synthesized by Sol-Gel process in the photocatalysis process. For the coagulation-flocculation process, organic (chitosan) and inorganic (aluminum sulfate) coagulants were used. As phenol is one of the harmful contaminants in vinasse, we also have focused on the degradation of this compound. Finally, in order to determinate if the pollutants were significantly reduced after the treatments, an analysis of variance (ANOVA) was carried out.

## *2. Material and methods*

### *2.1. Synthesis of $TiO_2$ nanoparticles.*

The synthesis of $TiO_2$ nanoparticles was done mixing 4 mL of hydrochloric acid (HCl 37 %, Merck) with 78 mL of 2-propanol ($C_3H_8O$, ACS reagent ≥99.5 %, Sigma-Aldrich), the mix was stirred for some minutes and 8 mL of titanium tetraisopropoxide ($Ti(C_3H_6OH)_4$, 97 %, Sigma-Aldrich) was added drop-wise; then, 3 mL of ammonium hydroxide ($NH_4OH$, 28-30 %, Sigma-Aldrich) was added. After that, the mix was stirred for 24 h at 25°C, after which a white powder settled down in the beaker, from which, the solvent was evaporated at 80°C, finally the powder was collected and annealed in air at 400°C for 3 h [18,19]. The annealed powder was grounded in a mortar and was labeled as S7. This sample was characterized by X-ray diffraction (XRD) in a PANalytical Empyrean diffractometer unit, using CuKα radiation, (λ=1.546 Å). The crystallite size was calculated from XRD using the Scherrer equation. Ultraviolet-visible spectroscopy (UV-vis) was carried out in a 3600 Shimadzu spectrophotometer. The study of the morphology was done by transmission electron microscopy (TEM) in a Philips TECNAI-F30 HRTEM 300 kV unit using the mode of high angle annular dark-field. Particle diameters were measured with Gwyddion software (Department of Nanometrology, Czech Metrology Institute). Raman spectroscopy was done in a Thermo Scientific DXR unit using a laser of 633 nm.

*2.2. Tequila vinasse characterization.*

Tequila vinasse was supplied by the Tequila Regulatory Council (CRT, Zapopan, Jalisco, México) [20], and was stored in a closed container at 279 K. The physicochemical characterizations of raw and treated vinasse were done by measuring pH, conductivity, TSS ($mg.L^{-1}$), color (Pt-Co) and COD ($mg.L^{-1}$) in a colorimeter Hach DR 900.

*2.3. Treatment of tequila vinasse by coagulation-flocculation.*

The coagulation-flocculation tests were conducted in a jar test apparatus by using 200 mg of chitosan (organic coagulant-flocculant, CFo), or 4 g of aluminum sulfate ($Al_2(SO_4)_3.(14\text{-}18)H_2O$), inorganic coagulant-flocculant, CFi) per 1000 mL of vinasse. In addition, in both cases, calcium hydroxide ($Ca(OH)_2$) was used as a sedimentation agent in doses of 4 and 6 g per 1000 mL of vinasse. The dose of coagulant-floculant was selected first, based on previous studies with other effluents [21,22] and then it was varied until finding the optimal values for the vinasse treatment. The vinasse treated by coagulation-flocculation process was identified as clarified vinasse. The conditions and description of these processes are summarized in Table 1. Subsequently, 200 mL of clarified vinasse was taken, to be treated by heterogeneous photocatalysis. After coagulation-floculation process, aliquots of 10 mL were taken for color and TSS analysis; 2 mL samples also were taken for COD test. These parameters were determined as described in the Standard Methods for the examination of water and wastewater [23]. In addition, the reduction of phenol concentration was followed by gas chromatography (GC).
[Table 1 near here]

*2.4. Heterogeneous photocatalysis*

A 1000 mL Pyrex beaker was used as batch photo-reactor for the study of the

photocatalysis process. The illumination was done with a 20 W black light lamp (365 nm wavelength), with an irradiance of 3.4 $W.m^{-2}$, which was measured with a pyranometer LICOR PY52668. The lamp was supported at 3 cm over clarified vinasse with universal bracket, and the whole was wrapped with aluminum foil to prevent UV light losses. For each experiment, a volume of 200 mL of clarified vinasse was used and a different quantity of S7 $TiO_2$ was added, i.e., 50, 100, 200, 400, and 600 mg. Additionally, in other experiment, 200 mg of commercial $TiO_2$ nanoparticles (Sigma-Aldrich, < 25 nm of particle size, 99.7 %, anatase) was also added, in order to evaluate its efficiency and compare it with those obtained with S7 $TiO_2$; this sample was identified as CA. After the addition of $TiO_2$, 2 mL of hydrogen peroxide ($H_2O_2$) was added to the reactor, and the samples were irradiated for 3 h, in order to carry out the photodegradation process. The time of irradiation and volume of $H_2O_2$ as well as the amount of nanoparticles we used to obtain the highest efficiency were found after varying those values reported in previous studies, [16,24]. After the determination of the optimal quantity of synthesized $TiO_2$ nanoparticles and time of treatment, a test was performed with commercial $TiO_2$ in the optimal conditions. The initial and final temperature of the reaction medium was 298 K and 302 K, respectively. The samples inside the reactor were stirred magnetically throughout the photocatalytic process (Figure 1). When the time was completed, aliquots of 10 mL were taken for color and TSS analysis; and aliquots of 2 mL were also taken for COD tests. These parameters were determined as described in *2.3*. Furthermore, the treated vinasse was analyzed by UV-vis and Raman spectroscopy, as well as by GC in order to determine the concentration of harmful compounds such as phenol.
[Figure 1 near here]

The influence of several factors such as the effect of photolysis, volume of $H_2O_2$, the mass of nanoparticles, time of treatment, etc. were evaluated; all the information with regard to these factors is summarized in Table 2.
[Table 2 near here]

*2.5. Analysis of phenol by gas chromatography coupled with mass spectrometry*

The GC measurements were conducted to determine phenol in tequila vinasse without treatment (Test 1) and after treatments 13 and 15 (see Table 2). Organic compounds were determined by GC coupled with mass spectrometry following methods used for alcoholic beverages. The identification of the principal compounds was done, comparing the peaks of chromatographic mass spectra with the total ion chromatograms. Were used standards in the quantification of compounds, samples and standards were analyzed according to the methodology of Mancilla-Margali and López (2002) [25] and every sample was analyzed by duplicate.

*2.6. Analysis of variance.*

In order to determine if there were significant differences ($p \leq 0.05$) between the results of tequila vinasse treatments, one-way analysis of variance (ANOVA) was performed in all the tests, taking COD, color, and SST as dependent variables. The analysis was performed using Statgraphics Centurion XVI software.

## 3. Results and discussion

### 3.1. Characterization of $TiO_2$ nanoparticles.

Figure 2 shows XRD of S7 (with and without treatment) and CA samples. In the S7 sample without treatment, the presence of $NH_4Cl$ was found, which is synthesized according to the reaction 1 and decomposes at 340°C into a mixture of two colorless gases, ammonia and hydrogen chloride [18].

$$HCl + NH_4OH \rightarrow NH_4Cl + H_2O \qquad (1)$$

For the CA sample, anatase phase diffractions at 25.4°, 37.9°, 48.1°, 53.9°, 55.0°, 62.2° and 68.9° were found, which are related to the planes (101), (004), (200), (105), (211), (213), and (116), respectively. The same diffractions were observed for the annealed S7 sample and also, a small contribution of the rutile phase at 27.4° (plane 110) was observed [26,27,25,29]. Scherrer equation (Equation 2) [26] was used to calculate the crystallite size, resulting in values of 18 and 9.8 nm for CA and S7, respectively.

$$d=(K\lambda)/(\beta\cos\theta) \qquad (2)$$

**$d$ is the crystallite diameter, $K$ is a dimensionless shape factor, with a value close to unity. The shape factor has a typical value of about 0.9, but varies with the actual shape of the crystallite, $\lambda$ is the wavelength of Cu K-alpha, (0.15418 nm), $\beta$ is the full width at half maximum of the highest diffraction in radians (plane 101), and θ is the Bragg angle in degrees. By using the Equation 3 [4] it was possible to calculate the composition of the anatase-rutile mix of the annealed S7 sample, which were 94.4 and 5.6 %, respectively; while CA sample showed a composition of 100 % anatase. In Equation 3, $I_R$ and $I_A$ are the diffraction peak intensities of the anatase and rutile phases, and K=0.79 [4]. From previous reports it is known that the anatase phase shows high photocatalytic activity [30], but when a mix of anatase-rutile with a higher concentration of anatase is used, the photocatalysis efficiency is increased [31,32,33].**

$$X_R=[K\,(I_R/I_A)]/[K\,(I_R/I_A)+1] \qquad (3)$$

[Figure 2 near here]

Figure 3 shows a TEM image of the S7 and CA sample, the nanoparticles showed a spherical shape and were agglomerated and a representative size of ~9.7 nm and 22.5 nm, respectively was found. For the case of S7 these results showed that the grain size and crystallite size were similar. Nanoparticles of samples S7 and CA showed polycrystalline structures, showing higher proportion of the anatase phase.
[Figure 3 near here]

Figure 4 shows Raman spectroscopy of $TiO_2$ without thermal treatment (a), annealed S7 (b) and CA (c). S7 and CA samples showed bands characteristic of anatase phase at 144 $cm^{-1}$($E_{og}$), 400 $cm^{-1}$($B_{1g}$), 505 $cm^{-1}$($A_{1g}$) and 640 $cm^{-1}$($E_{og}$) [34]. There was also congruency in the results of $TiO_2$ without annealing, as Raman spectroscopy showed the spectrum characteristic of $NH_4Cl$ compound [35].
[Figure 4 near here]

Figure 5 shows UV-vis spectra of S7 and CA samples. For S7, and CA, the light absorption was in the UV-vis region, (<500 nm); in this way the materials are stimulated with photons with enough energy to produce electron-hole pairs and electron transitions from the valence band to the conduction band [36,37]. The band gap was calculated by extrapolation of the linear part of the graph of $(\alpha h\nu)^2$ versus energy, resulting in 3.03 and 3.13 eV for S7, and CA respectively, in line with previous reports [27].
[Figure 5 near here]

### *3.2. Characterization of raw vinasse*

Table 3 shows the physicochemical characteristics of raw tequila vinasse. The high concentrations of COD, TSS, and color, are due to the presence of organic and inorganic materials, as well as phenolic compounds, which come from the *Agave tequilana*. Phenolic compounds is a group of micronutrients also called secondary metabolites and includes polyphenols, tannins, flavonoids, and lignins [38,39]. The reaction of the phenolic compounds with sugar and aminoacids (also present in tequila vinasse) at alkaline pH and high temperature is known as the Maillard reaction, such reaction, generates melanoidin, which is responsible for the characteristic dark brown color of the vinasse [4,40-42].
[Table 3 near here]

### *3.3. Treatment of tequila vinasse by coagulation-flocculation and heterogeneous photocatalysis*

The general process of photocatalysis is described in the reactions 4-8. Photons with enough energy hit the $TiO_2$ and produce electron-hole pairs, (holes in valence bands and electrons in conduction bands), holes produce ·OH radicals with high oxidative potential, which in turn oxidize and degrade organic substances.

$$TiO_2 + h\nu \rightarrow e^-_{cb} + h^+_{vb} \quad (4)$$

$$h^+_{vb} + H_2O \rightarrow H^+ + \bullet OH \quad (5)$$

$$h^+_{vb} + OH^- \rightarrow \bullet OH \quad (6)$$

$$Organic\ sustance + \bullet OH \rightarrow degradation\ products \quad (7)$$

$$Organic\ sustance + h_{vb}^{+} \rightarrow degradation\ products \quad (8)$$

Figure 6 shows the results in the reduction of TSS, color, and COD, due to the different treatments (see Table 2). From the ANOVA it was determined that the differences amongst all the treatments were statistically significant (p-value < 0.05).

The efficiency of photolysis in the reduction of TSS, color, and COD (Test 2) was very low; therefore photolysis could be discarded as an important step in the treatment. With respect to the coagulation-flocculation processes, the inorganic coagulant was more effective (Test 7) in comparison to the organic coagulant (Test 6). The results of Test 7 were similar to those in previous reports obtained for sugarcane vinasse [16]. Regarding the mass of $TiO_2$ nanoparticles, several amounts in the range from 50 to 600 mg were tested, being 200 mg the most effective. Apparently, higher amounts produced shielding effects to the light [43,44], while lower concentrations were not enough to produce the desirable effects. With regard to photocatalysis, two assays were done with 3 h (Test 13), and 24 h (Test 14). From these assays, photocatalysis with 3 h was selected because there was not a significant difference in comparison to the assay with 24 h. With 3 h, the decrease in TSS, color and COD were 99.4 %, 86.0 % and 70.0%, respectively. Previous investigations reported reductions of color, and COD of 87 and 80% respectively with times of 40 and 48 h [4]. Regarding the efficiency of the process as a function of the type of nanoparticles, it was found that the nanoparticles synthesized in our laboratory (S7) showed the highest efficiency, especially for the reduction of color, and COD. Some reasons for the superior performance of S7 could have been the higher surface area as a result of the smaller grain size, the mix anatase-rutile [4], and/or the fact that most of S7 and CA nanoparticles were polycrystalline as was observed in XRD and TEM. The last reason could be more important, because in this sample, in addition to the higher surface area we had the maximum surface area available per gram, assuming that the grain size is the same than crystal size.

[Figure 6 near here]

### *3.4. UV-vis, Raman spectroscopy and gas chromatography analysis of the treated vinasse*

Figure 7 shows the absorbance after some treatments; the absorption band was located in the range from 200 to 600 nm, with the maximum at 280 nm. The peak of maximum absorbance has been related to the presence of organic compounds such as furfural, 5-methyl furfural and 2-acetyl furan [45]. These compounds almost disappeared as the samples underwent heterogeneous photocatalysis; the reduction was strongest for samples treated with S7 nanoparticles, in line with the previous characterization.

[Figure 7 near here]

Figure 8 shows Raman spectroscopy of raw vinasse before and after treatments. It was a little difficult to identify all the vibrational modes given the high quantity of components in tequila vinasse; however, most of the Raman signals could be attributed to ethanol, acetic acid, and glycerol. The following analysis is from lower to higher wave numbers. In the frequency range of 700-1500 $cm^{-1}$, the broad and intense signal could be attributed to ethanol functional groups containing the bonds -C-C, C-O, $-CH_2$ and $–CH_3$, specifically, the stretching vibration of -C-C (883 $cm^{-1}$), the stretching

vibration of -C-O group (1054 $cm^{-1}$), and the rocking vibration of the $CH_3$ group (1096 $cm^{-1}$) [46], at 1454 $cm^{-1}$ we could have the bands corresponding to the groups $–CH_2$ and $–CH_3$, as well as the asymmetrical stretching of acetate salt $COO^-$(1550-1610 $cm^{-1}$) [47]. In the range from 1300 to 2300 $cm^{-1}$ there is another group of signals that could be related to acetic acid, which, is in high concentration in tequila vinasse; signals in the range from 1780 to 1805 $cm^{-1}$ could be related to the stretching vibration of C=O bond, as well as to other functional groups related to $CH_3COOX$ (X≠carbon atom) (1710 to 1810 $cm^{-1}$) [47]. In the range 2550-2580 $cm^{-1}$, there was an intense peak related to the stretching of sulfhydryl group S-H; this group is present in thiols of some aminoacids. The stretching of C-H bond was found in the range 2850-2885 [48,49]. We also observed vibrations and stretching of •OH groups bonded to hydrogen at frequencies of 3420 and 3250 $cm^{-1}$ [50,51]. It was remarkable that all the bands decreased as the treatments were applied. When coagulation-flocculation process was applied, all the bands decreased, however when photocatalysis was applied, especially with S7 sample (Test 13), some bands (500-1000 $cm^{-1}$) disappeared completely, therefore, according to this result, photocatalysis process using $TiO_2$ nanoparticles synthesized in our laboratory is an efficient process for the treatment of tequila vinasse [37,52,53].
[Figure 8 near here]

Gas chromatography was used to determine phenol concentration in vinasse without treatment (1) and vinasse treated with photocatalysis using S7 (Test 13) and CA (Test 15). Phenol concentration in vinasse without treatment was 2.72 $mg.L^{-1}$; after the treatment, the concentration of (7), (13) and (15) samples was reduced to 1.46 $mg.L^{-1}$, 0.28 and 0.47 $mg.L^{-1}$ respectively, (see Figure 9), i.e., a reduction of 46.3 %, 89.7 % and 82.7 %. The chromatograms of these analyses are shown in Figure 10. It was clear the difference between treatments (13) and (15), which demonstrates the effectiveness of using S7 $TiO_2$ nanoparticles. The reduction of phenol was due to the photocatalytic oxidation by means of an electrophilic attack by hydroxyl radicals, producing the hydroxylation of the benzene ring; during this process, intermediate products such as hydroquinone, catechol, and benzoquinone are generated, as well as products like carboxylic acids, malonic acid, organics acids of short-chain like maleic acid, oxalic acid, acetic acid and formic acid along with carbon dioxide and water [37,52,53]. According to GC results the compounds that were generated during the treatment of tequila vinasse by heterogeneous photocatalysis were ethylene glycol and acetaldehyde. Although glycerol, acetic acid, formic acid and butanoic acid were present in raw tequila vinasse and in the treated tequila vinasse, we do not know if there was an increase by heterogeneous photocatalysis. So that, it was not possible to confirm if their presence in the treated tequila vinasse was due to their initial presence in the raw vinasse or was due to their formation during the treatment. The majority of these compounds are shown in figure 10 and in the table 4, with their respective concentrations and abundance time.
[Figure 9 and 10 near here]
[Table 4 near here]

## 4. Conclusions

It was possible to treat raw tequila vinasse by coagulation-flocculation coupled with heterogeneous photocatalysis. We also have synthesized and characterized reactive titanium dioxide nanoparticles which were able to decompose chemical pollutants present in tequila vinasse by photocatalysis, with higher efficiency than the commercial

ones. There was a considerable reduction in the pollutant concentrations after the coagulation-flocculation process, up to over half of the initial concentrations; however with this process, there were no evidence of chemical degradation of the pollutants. For that purpose, titanium dioxide nanoparticles performed well, specifically nanoparticles synthesized in our laboratory. It was remarkable that nanoparticles were able of degrading almost completely, harmful pollutants such as phenol. Using several analytical techniques it was possible to quantify the decontamination level, so that we concluded that coagulation-flocculation process coupled with heterogeneous photocatalysis could be used as an alternative to solve the serious environmental issue of tequila vinasse.

**Acknowledgements**

We acknowledge the funding from projects Ciencia Básica 167833 SEP-CONACYT, Infraestructura Científica y Tecnológica 279937 CONACYT, México, to the funding of Fortalecimiento de la Investigación y el Posgrado de la UdeG for their support through Grant No. CV/XVI/32/2017 and for the scholarship of Alicia Rodriguez Arreola.

**References**

[1] Cedeño M. Tequila production. Crit. Rev. Biotechnol. 1995;15:1-11.

[2] Colin VL, Cortes AAJ, Aparicio JD, Amoroso MJ. Potential application of a bioemulsifier-producing actinobacterium for treatment of vinasse. Chemosphere. 2016;144:842-847.

[3] López A, Contreras SM. Ciencia y tecnología, Guadalajara, Jalisco, Capítulo 8: Tratamiento de efluentes y aprovechamiento de residuos, segunda edición Grupo Promueve, Guadalajara, Jalisco. 2015:343-378.

[4] Padilha de Souza R, Ferrari AM, Pezoti O, et al. Photodegradation of sugarcane vinasse: evaluation of the effect of vinasse pre-treatment and the crystalline phase of $TiO_2$. Acta Sci.-Technol. 2016;38:217-226.

[5] Santana V, Fernandes NRC. Photocatalytic degradation of the vinasse under solar radiation. Catalysis Today. 2008;133-135:606-610.

[6] Moran RG, Sanchez AL, Rodriguez J, et al. Utilization of vinasses as soil amendment: consequences and perspectives. Springer Plus. 2016;5:1-11.

[7] Ferral H, Bustillos LG, Mendez H, et al. Sequential treatment of tequila industry vinasses by biopolymer based coagulation/flocculation and catalytic ozonation. Ozone-Sci. Eng. 2016;38:279-290.

[8] Harada H, Uemera S, Cheng A, et al. Anaerobic Treatment of a recalcitrant distillery wastewater by a thermophilic UASB reactor. Bioresource Technol. 1996;55:215-221.

[9] Alonso V, Martín A, Borja R. Anaerobic digestion of wastewater produced in the manufacture of cellulosic pulp from wheat straw in immobilized cell bioreactors. Resour. Conserv.Recy. 1995;13:129-138.

[10] Zayas T, Salgado VRVRL, Meraz M, et al. Applicability of coagulation/flocculation and electrochemical processes to the purification of biologically treated vinasse effluent, Sep. Purif. technol. 2007;57:270-276.

[11] Riga ACK, Soutsasb K, Karayannisa V, et al. Effect of system parameters and of inorganic salts on the decolorization and degradation of Procion H-exl dyes. Comparison of $H_2O_2$/UV, Fenton, UV/Fenton, $TiO_2$/UV and $TiO_2$/UV/$H_2O_2$ proceses. Desalination. 2007;211:72-86.

[12] Navarro P, Sarasa J, Sierra D, et al. Degradation of wine industry wastewaters by photocatalytic advanced oxidation. Water Sci. Technol. 2005;51:113-20.

[13] Zhang H, Liu G, Shi L, et al. Engineering coordination polymers for photocatalysis. Nano Energy. 2016;22:149-168.

[14] Herrmann JM, Guillard C, Pichat P. Heterogeneous photocatalysis: an emerging technology for water treatment. Catal. Today. 1993;17:7-20.

[15] Matos J, Miranda C, Poon PS, et al. Nanostructured hybrid $TiO_2$-C for the photocatalytic conversion of phenol. Sol. Energy. 2016;134:64-71.

[16] Padilha de Souza R, Girardi F, Sluzarski V, et al. Vinasse treatment using a vegetable-tannin coagulant and photocatalysis. Acta Sci.-Technol. 2013;35(1):89-95.

[17] Vineetha MN, Matheswaran M, Sheeba KN. Photocatalytic colour and COD removal in the distillery effluent by solar radiation. Sol. Energy. 2013;91:368-373.

[18] Sánchez M, Guirado R, Rincón ME. Desarrollo y caracterización de un composito basado en dióxido de titanio y nanotubos de carbono para su aplicación como sensor de gases tóxicos (tesis de maestría). Centro de Investigación en Energía de la Universidad Autónoma de México, Temixco, Morelos. 2006.

[19] Sanchez M, Guirado R, Rincón ME. Multi walled carbon nanotubes embedded in sol-gel derived $TiO_2$ matrices and their use as room temperature gas sensors. J. Mater Sci: Mater Electron. 2007;18:1131-1136.

[20] https://www.crt.org.mx/index.php?lang=en

[21] Selmer E, Ratnaweera HC, Pehrson R. A novel treatment process for dairy wastewater with chitosan produced from shrimp shell waste. Wat. Sci. Tech. 1996;34(11):33-40.

[22] Lalov IG, Guerginov II, Krysteva MA, et al. Treatment of waste water from distilleries with chitosan. Wat. Res. 2000;34(5):1503-1506.

[23] American Public Health Association; American Water Works Association; Water Environment Federation. Standard Methods for the Examination of Water and Wastewater, 21st ed.; American Public Health Association: Washington, DC, USA, 2005.

[24] Wei TY, Wan CC. Heterogeneous photocatalytic oxidation of phenol with titanium dioxide powders. Ind. Eng. Chem. Res. 1991;30(6):1293-1300.

[25] Mancilla-Margalli NA, López MG. Generation of Maillard compounds from inulin during the termal processing of Agave tequilana Weber Var. azul. J. Agric. Food Chem. 2002;50(4):806-12.

[26] Zhang H, Baffled JF. Understanding polymorphic phase transformation behavior during growth of nanocrystalline aggregates: Insights from $TiO_2$. J. Phys. Chem. B. 2000;104:3481-3487.

[27] Hernández JM, García LA, Zeifert BH. Síntesis y caracterización de nanopartículas de N-$TiO_2$-Anatasa. Superficies y Vacío. 2008;21:1-5.

[28] Bizarro M, Tapia MA, Ojeda ML, et al. Photocatalytic activity enhancement of $TiO_2$ films by micro and nano-structured surface modification. Appl. Surf. Sci. 2009;255:6274-6278.

[29] Giuliante A, Marrero S, Carrillo V, et al. Physico-chemical properties of La/$TiO_2$ systems employed for 2-nitrophenol photodegradation using visible light from a solar simulator. Rev. Fac. Ing. UCV. 2011;26:147-154.

[30] Tayade RJ, Surolia PK, Kulkarni RG, et al. Photocatalytic degradation of dyes and organic contaminants in water using nanocrystalline anatase and rutile TiO2. Sci. Technol. Adv. Materials. 2007;8:455-462.

[31] Bacsa RR, Kiwi J. Effect of rutile phase on the photocatalytic properties of nanocrystallinetitania during the degradation of p-coumaric acid. Appl. Catal. B-Environ. 1998;16:19-29.

[32] Hou H, Shang M, Wang L, et al. Efficient photocatalytic activities of $TiO_2$ hollow fibers with mixed phases and mesoporous walls. Scientific Reports. 2015;5:1-9.

[33] Ruu W, Lintang HO, Shamsuddin M, et al. High photocatalytic activity of mixed anatase-rutile phases on commercial $TiO_2$ nanoparticles. IOP Conf. Series: Materials Science and Engineering. 2016;107:1-8.

[34] Capula SI. Síntesis, caracterización y evaluación de la actividad catalítica de nanopartículas Pt-Ir sobre nanotubos de titania. Tesis. 2007:1-78.

[35] OMNIC spectra software, ThermoFisher Scientific

[36] Zhang YX, Li GH, Jin YX, et al. Hydrothermal synthesis and photoluminescence of $TiO_2$ nanowires. Chem. Phys. Lett. 2002;365:300-304.

[37] Henderson MAA. Surface science perspective on $TiO_2$ photocatalysis. Surf. Sci. Rep. 2011;66:185-297.

[38] Lotero ML. Transformaciones del carbono orgánico presente en la vinaza aplicada a un suelo vertic haplustoll de Valle de Río Cauca (tesis doctoral), Universidad Nacional de Colombia, Palmira, Colombia. 2012.

[39] Ortiz M, Solis E. Procedimiento, aditivos y formulación para el tratamiento de vinazas. Search International and National Patent Collections. 2012.

[40] Reynolds TM. Chemistry of non enzymic browing. I. The reaction between aldoses and amines. Adv. Food Res. 1968;12:1-52.

[41] http://depa.fquim.unam.mx/amyd/archivero/07LareacciondeMaillard_20547.pdf

[42] Tamanna N, Mahmood N. Food processing and Maillard reaction products: Effect on human health and nutrition. International Journal of Food Science. 2015;2015:1-6.

[43] Giratá LM, Guevara JE, Machuca F. Exploring Study on the Vinasse Treatment by Solar Photocatalysis with Titanium Dioxide in a Falling Film Reactor. Rev. ION. 2011;24:35-41.

[44] Konstantinou IK, Albanis TA. TiO2-assisted photocatalytic degradation of azo dyes in aqueous solution: kinetic and mechanistic investigations A review. Appl. Catal. B-Environ. 2004;49:1-14.

[45] Contreras U, Barbosa O, Ramos G, et al. Identificación y discriminación de tequilas reposados in situ para la protección de marca. Nova Sci. 2009;1:22-32.

[46] Picard DI, Montagnac G, Oger P. In situ monitoring by quantitative Raman spectroscopy of alcoholic fermentation by Saccharomyces cerevisiae under high pressure. Extremophiles. 2009;11:445-452.

[47] Socrates G. Infrared and Raman characteristic group frequencies. Tables and charts. England. Jhon Wiley & Sons. LTD. 2001.

[48] Limem S, Maazaoui R, Mani KD, et al. Preliminary identification of citrullus colocynthis from Togo by FT-IR and Raman spectroscopy. International Journal of Advanced Research. 2015;3:354-360.

[49] Schulz H, Baranska M. Identification and quantification of valuable plant substances by IR and Raman spectroscopy. Vibrational Spectroscopy. 2007;43:13-25.

[50] Tyrode E, Magnus C, Baldelli S, et al. A vibrational sum frequency spectroscopy study of the liquid- gas interface of acetic acid-water mixtures: 2. Orientationanalysis. J. Phys. Chem. B. 2005;109:329-341.

[51] Frausto C, Medina C, Sato R, et al. Qualitative study of ethanol content in tequilas by Raman spectroscopy and principal component analysis. Spectrochim Acta A. 2005;61:2657-2662.

[52] Grabowska E, Reszczynska J, Zaleska A. Mechanism of phenol photodegradation in the presence of pure and modified-$TiO_2$: A review. Water Research. 2012;46:5453-5471.

[53] Sobczyynski A, Duczmal L, Zmudzinski W. Phenol destruction by photocatalysis on $TiO_2$: an attempt to solve the reaction mechanism. Journal of Molecular Catalysis A: Chemical. 2004;213:225-230.

[54] Fan W, Qlan MC. Headspace solid phase microextraction and gas chromatography olfactometry dilution analysis of Young and aged chinese “Yanghe Daqu” liquors. J. Agric. Food Chem. 2005;53:7931-7938.

[55] Dowd MK, Johansen SL, Cantarella L, et al. Low molecular weight organic composition of etanol stillage from sugarcane molasses, citrus waste, and sweet whey. J. Agric. Food Chem. 1994;42:283-288.

[56] Gallego CM. Influencia de la acidez volatile en el proceso de fermentación de la planta de alcohol del ingenio Risaralda, S.A. (tesis de grado), Universidad Tecnológica de Pereira, Colombia. 2007.

[57] Ralph J, Hatfield RD. Pyrolisis GC-MS characterization of forage materials. J. Agric. Food Chem. 1991;39:1426-1437.



Table 1.

| | Coagulant CFi | Coagulant CFo |
|---|---|---|
| Tequila vinasse (mL) | 1000 | 1000 |
| $Al_2(SO4)_3$. (14-18)$H_2O$ (mg) | 4000 | |
| Chitosan (mg) | | 200 |
| Initial stirring speed (rpm) | 225 | 225 |
| Initial stirring time (min) | 5 | 5 |
| Final stirring speed (rpm) | 60 | 60 |
| Stirring time (min) | 60 | 60 |
| $Ca(OH)_2$ (mg) | 6000 | 4000 |
| Initial stirring speed (rpm) | 125 | 125 |
| Stirring time (min) | 5 | 5 |
| Final stirring speed (rpm) | 60 | 60 |
| Stirring time (min) | 30 | 30 |
| Sedimentation time | 60 | 60 |

(min)

Table 2.

| Test | UV light exposure time (h) | $H_2O_2$ (mL) | S7 (mg) | CA (mg) | Coagulation-flocculation |
|---|---|---|---|---|---|
| 1 | | | | | |
| 2 | 3 | | | | |
| 3 | | 2 | | | |
| 4 | 3 | 2 | | | |
| 5 | 3 | | 200 | | |
| 6 | | | | | Organic (CFo): 200 mg chitosan + 4g $Ca(OH)_2$ |
| 7 | | | | | Inorganic (CFi): 4g $Al_2(SO_4)_3.(14\text{-}18)H_2O$ + 6g $Ca(OH)_2$ |
| 8 | 3 | | 200 | | CFi |
| 9 | 3 | 2 | 50 | | CFi |
| 10 | 3 | 2 | 400 | | CFi |
| 11 | 3 | 2 | 600 | | CFi |
| 12 | 3 | 2 | 100 | | CFi |
| 13 | 3 | 2 | 200 | | CFi |
| 14 | 24 | 2 | 200 | | CFi |
| 15 | 3 | 2 | | 200 | CFi |

Table 3.

| Parameter | Raw tequila vinasse |
|---|---|
| pH (units of pH) | 3.56 ± 0.006 |
| Conductivity ($\mu S.cm^{-1}$) | 2.33 ± 0.008 |
| TSS($mg.L^{-1}$) | 17,000 ± 20.000 |
| Color (Pt-Co) | 22,200 ± 12.500 |
| COD ($mg.L^{-1}$) | 35,600 ± 23.100 |
| Phenol ($mg.L^{-1}$) | 2.72 ± 0.000 |

**Table 4.**

| Tests | | (1) | (7) | (13) | (15) |
|---|---|---|---|---|---|
| Compounds | Time (min) | ppm | ppm | ppm | ppm |
| A) Acetaldehyde | 2.20 | – | 18.30 ± 0.92 | – | – |
| B) Butanoic acid | 8.54 | 4.94 ± 0.25 | 1.789 ± 0.09 | – | 1.07 ± 0.05 |

| | | | | | |
|---|---|---|---|---|---|
| C) Ethylene glycol | 9.78 | 16.88 ± 0.84 | 17.81 ± 0.89 | 2.19 ± 0.11 | 31.96 ± 1.60 |
| D) Acetic acid | 4.122 | 571.07 ± 28.55 | 446.69 ± 22.33 | 111.88 ± 5.60 | 202.62 ± 10.13 |
| E) Phenol | 22.33 | 2.72 ± 0.14 | 1.46 ± 0.07 | 0.28 ± 0.014 | 0.47 ± 0.02 |
| F) Glycerol | 30.44 | 668.33 ± 33.42 | 2738.86 ± 136.94 | 290.54 ± 14.53 | 1410.66 ± 70.53 |

- Where: _ No presence.

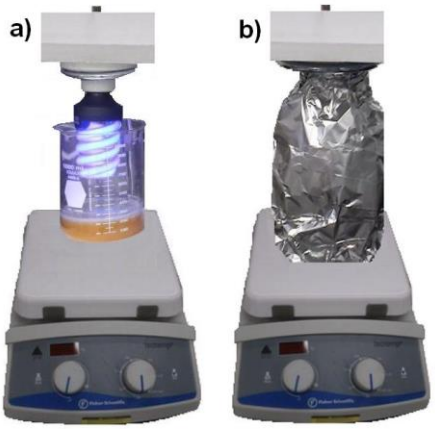


Figure 1.

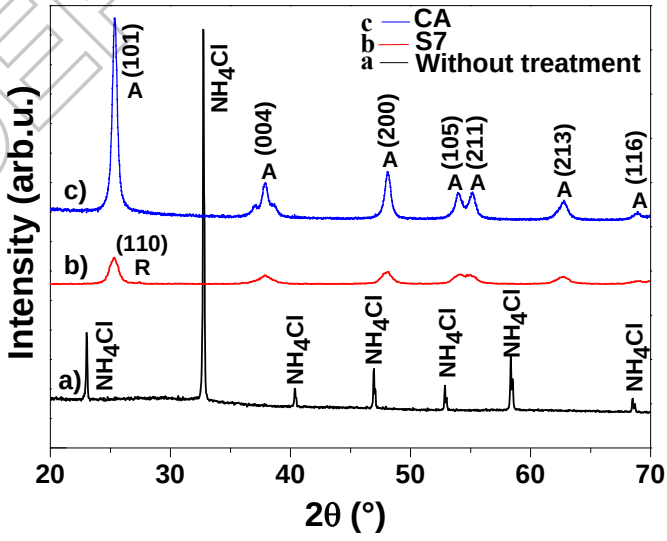

Figure 2.

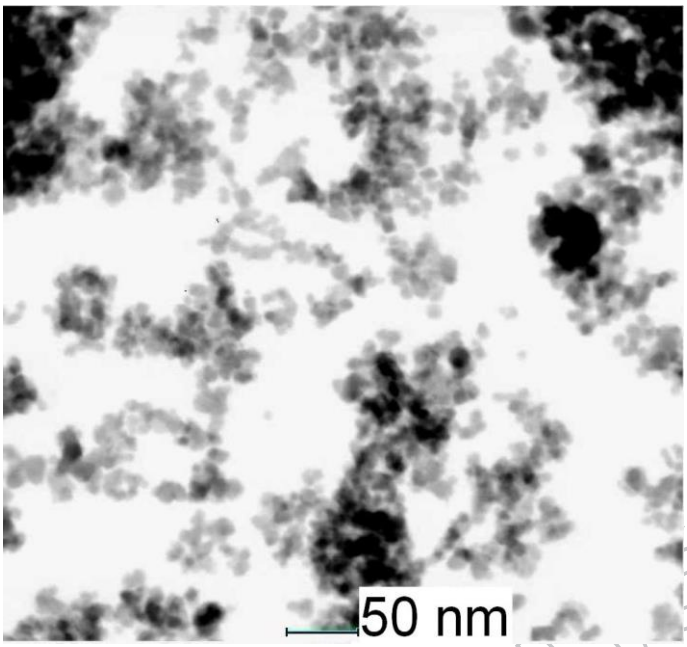


a)

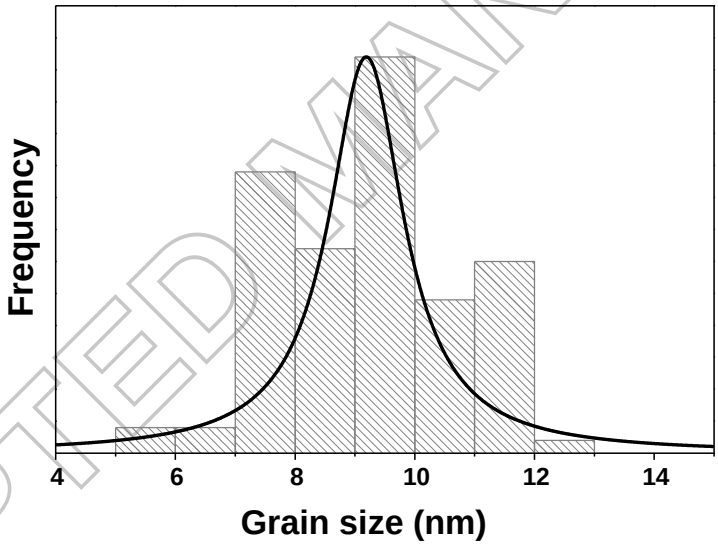


b)

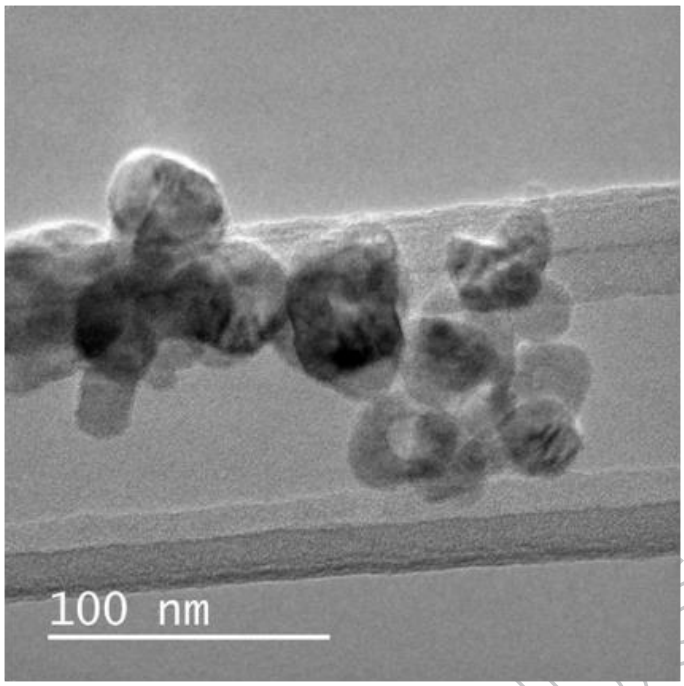


c)

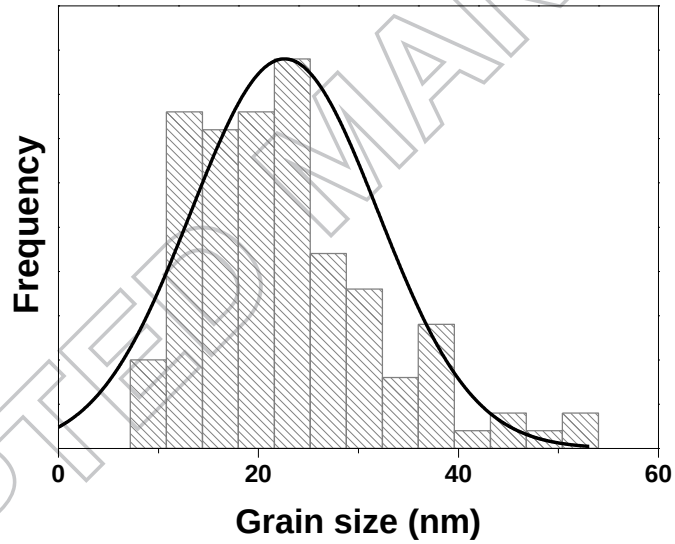


d)

Figure 3.

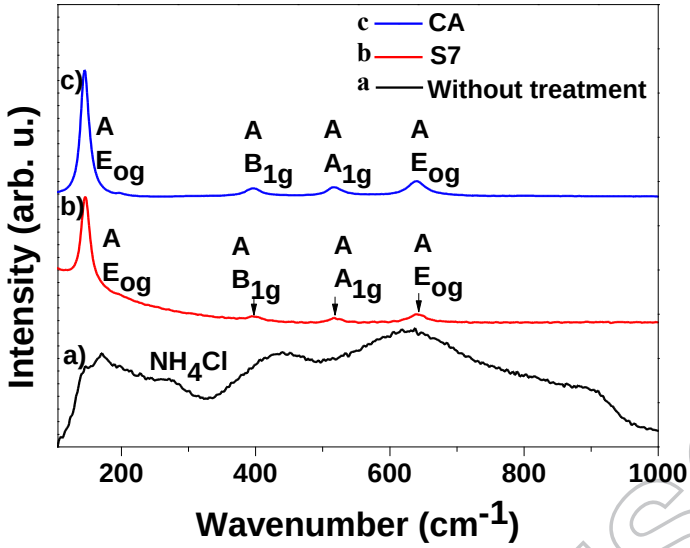


Figure 4.

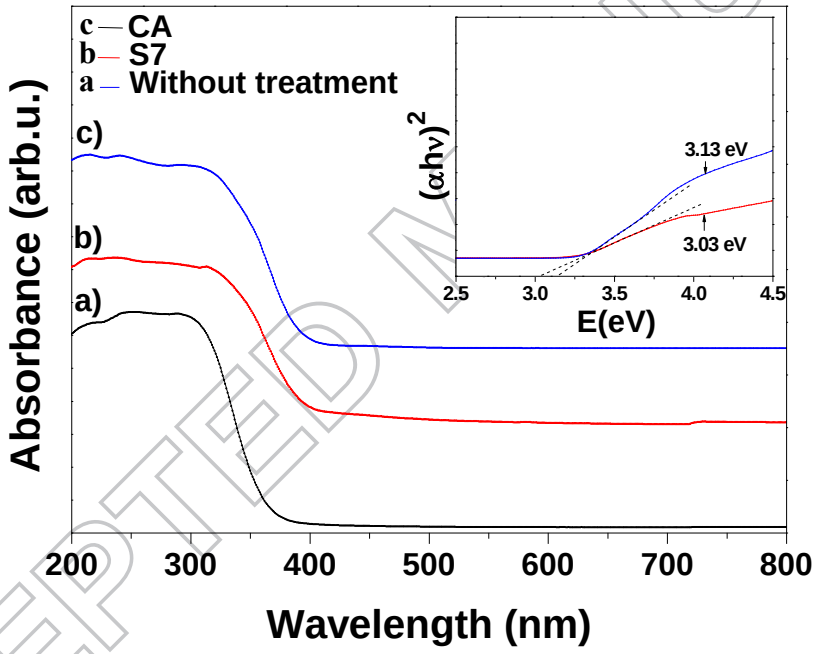


Figure 5.

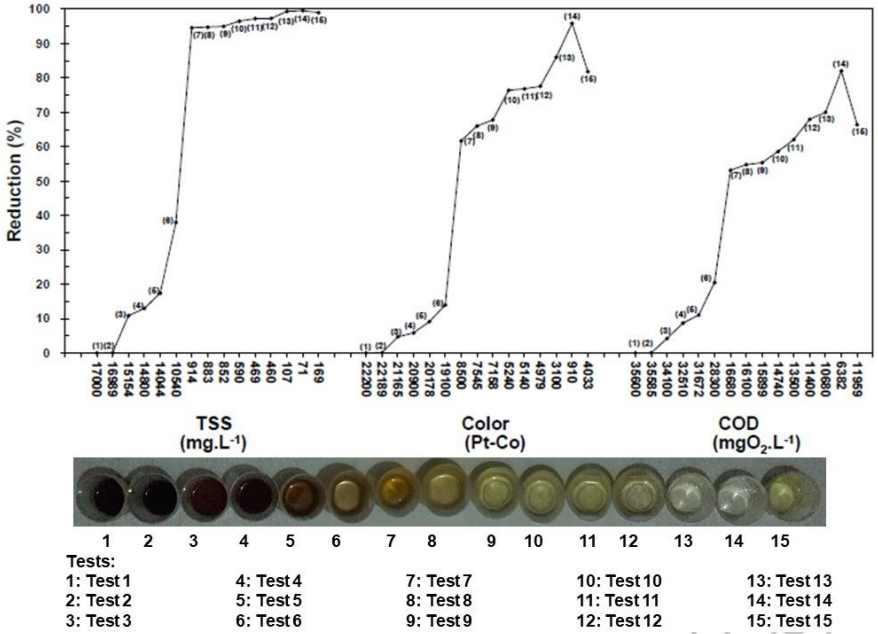


Figure 6.

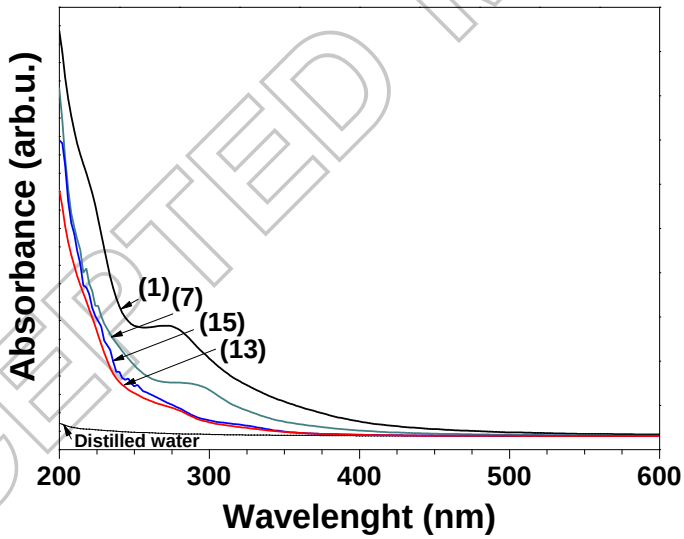


Figure 7.

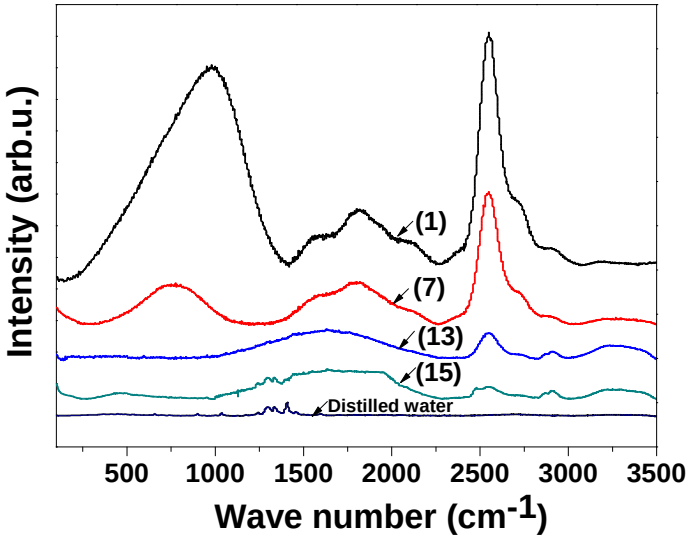


Figure 8.

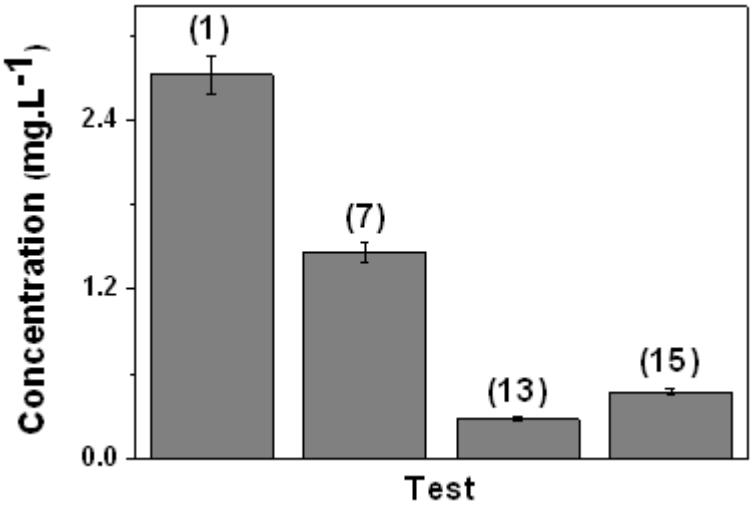


Figure 9.

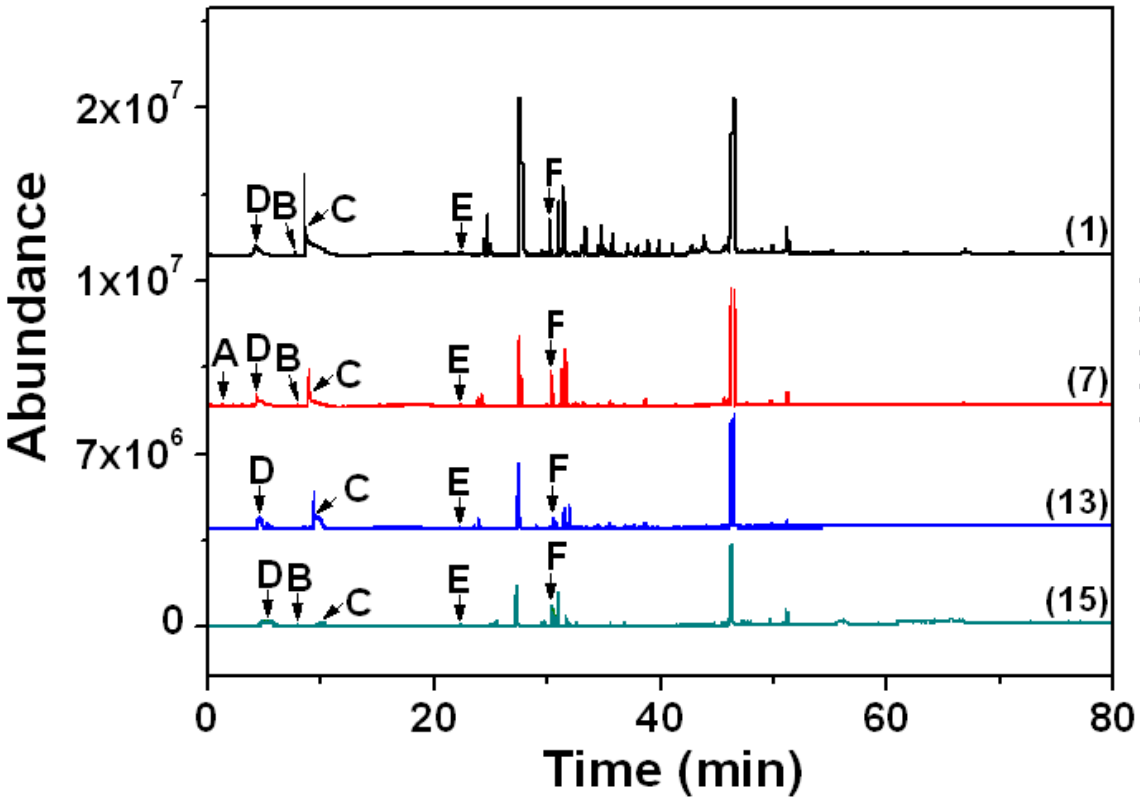


Figure 10

Table 1. Coagulation-flocculation process of tequila vinasse.

Figure 1. Experimental setup for heterogeneous photocatalysis: a) batch reactor with clarified tequila vinasse; b) reactor covered with aluminum foil.

Table 2. Different conditions of operations used in the treatment of tequila vinasse; samples of 200 mL of raw vinasse were used in all the tests.

Figure 2. XRD of a) $TiO_2$ without annealing, b) S7, and c) CA; A stand for anatase and R stands for rutile.

Figure 3. TEM image of S7 and CA $TiO_2$ powder, a) image S7, b) grain size of S7 distribution, c) image CA, d) grain size of CA distribution.

Figure 4. Raman spectroscopy of $TiO_2$ without annealing, S7, and CA powders; A: anatase. B: rutile.

Figure 5. UV-vis spectra of $TiO_2$: a) Without annealing, b) S7, and c) CA powders, the inset shows the calculation of band gap.

Table 3. Physicochemical characteristics of tequila vinasse used in this study.

Figure 6. Efficiencies of vinasse treatments in the reduction of TSS, color, and COD, and aspects of the solutions after the treatments.

Figure 7. UV-vis spectra of raw and treated vinasse, raw vinasse (Test 1), coagulation-flocculation (Test 7), heterogeneous photocatalysis using S7 (Test 13), heterogeneous photocatalysis using CA (Test 15), the black line corresponds to distilled water used as a blank.

Figure 8. Raman spectroscopy of raw tequila vinasse before and after treatments: raw vinasse (Test 1); vinasse treated by coagulation-flocculation (Test 7); vinasse treated by heterogeneous photocatalysis using S7 (Test 13), and CA (Test 15).

Figure 9. Phenol concentrations in tequila vinasse without treatment (Test 1), treated by coagulation flocculation (Test 7), heterogeneous photocatalysis using S7 (Test 13) and CA (Test 15).

Figure 10. Gas chromatography analysis of raw tequila vinasse (Test 1), treated by coagulation-floculation (Test 7), treated by heterogeneous photocatalysis using S7 (Test 13) and CA (Test 15). Where: A: Acetaldehyde, B: Butanoic acid, C: Ethylene glycol, D: Acetic acid, E: Phenol and F: Glycerol.

**Table 4.** Parameters obtained from the GC mass spectrograms of the tequila vinasse.